

General Binding Affinity Guidance for Diffusion Models in Structure-Based Drug Design

Yue Jian
UC Berkeley
yue_jian@berkeley.edu

Curtis Wu
UC Berkeley
curtis_wu@berkeley.edu

Danny Reidenbach
NVIDIA
dreidenbach@nvidia.com

Aditi S. Krishnapriyan
UC Berkeley
aditik1@berkeley.edu

Abstract

Structure-Based Drug Design (SBDD) focuses on generating valid ligands that strongly and specifically bind to a designated protein pocket. Several methods use machine learning for SBDD to generate these ligands in 3D space, conditioned on the structure of a desired protein pocket. Recently, diffusion models have shown success here by modeling the underlying distributions of atomic positions and types. While these methods are effective in considering the structural details of the protein pocket, they often fail to explicitly consider the binding affinity. Binding affinity characterizes how tightly the ligand binds to the protein pocket, and is measured by the change in free energy associated with the binding process. It is one of the most crucial metrics for benchmarking the effectiveness of the interaction between a ligand and protein pocket. To address this, we propose **BADGER: Binding Affinity Diffusion Guidance with Enhanced Refinement**. **BADGER** is a general guidance method to steer the diffusion sampling process towards improved protein-ligand binding, allowing us to adjust the distribution of the binding affinity between ligands and proteins. Our method is enabled by using a neural network (NN) to model the energy function, which is commonly approximated by AutoDock Vina (ADV). ADV’s energy function is non-differentiable, and estimates the affinity based on the interactions between a ligand and target protein receptor. By using a NN as a differentiable energy function proxy, we utilize the gradient of our learned energy function as a guidance method on top of any trained diffusion model. We show that our method improves the binding affinity of generated ligands to their protein receptors by up to 60%, significantly surpassing previous machine learning methods. We also show that our guidance method is flexible and can be easily applied to other diffusion-based SBDD frameworks.

1 Introduction

Structure-based drug design (SBDD) is a fundamental task in drug discovery, aimed at designing ligand molecules that have a high binding affinity to the receptor protein pocket [1, 2]. SBDD directly utilizes the three-dimensional structures of target proteins, enabling the design of molecules that can specifically interact with and influence the activity of these proteins, thus increasing the specificity and efficacy of potential drugs. The conventional workflow of SBDD consists of two key phases: “screening” and “scoring.” During the screening phase, a protein pocket is pre-selected and fixed, and a large database of ligand molecules is searched to find promising candidates. This phase is followed by the “scoring” phase, which involves either high-throughput experimental techniques or computational methods like molecular docking and Free Energy Perturbation (FEP). These methods evaluate and rank these candidates based on their predicted binding affinity to the target protein’s pocket [3, 4, 5].

The traditional SBDD workflow, while foundational, faces several challenges. First, high-throughput experimental techniques or computational methods are both time consuming and computationally demanding. Second, the search space for potential drug molecules is confined to the chemical database used in SBDD, limiting the diversity of candidates. Third, the optimization of candidate molecules post-identification is often influenced by human experience,

which can introduce biases. These issues highlight the need for more advanced computational solutions in SBDD to address these limitations effectively.

Recent advancements in machine learning, and particularly in generative modeling, have provided a computationally efficient alternative to the traditional SBDD approach. These developments can help overcome the limitations associated with the extensive ligand screening databases traditionally used in SBDD [6, 7, 8, 9, 10, 11]. Generative models use the protein pocket as a starting condition and design ligands from scratch. They model the latent distribution of ligand-protein pairs data, then generate valid ligands by sampling from this latent space and reconstructing the molecules with a trained decoder network. Among the various types of generative models used for SBDD, diffusion models have been particularly successful in generating ligands that have high binding affinity to their target protein pockets [12, 6, 13, 14].

Binding affinity is a key measure of how effectively a ligand interacts with a protein pocket. It is linked to essential properties for ligands, such as efficacy and selectivity as drug candidates. In practice, binding affinity is often approximated by AutoDock Vina’s energy function (denoted as ADV energy function), which is a scoring function based on atomic interactions [4]. Improving the binding affinity and quality of ligands generated by diffusion models has been a central focus of research in applying diffusion models to SBDD [6, 15, 13, 16, 17]. Recent works in this domain have shown success in improving the binding affinity of sampled ligands through various methods. However, each approach comes with its own set of challenges and limitations:

1. **Fragment-based method [13]:** This approach involves decomposing ligands into fragments and initializing their fragment positions with pre-designed priors before the sampling process. The effectiveness of this method depends heavily on the type and quality of the priors, which are tailored for specific families of pockets and ligands. This dependency makes it challenging to generalize the method to new types of ligands and pocket families.
2. **Filtering-based method [18]:** This method incorporates physics-based binding affinity predictors, such as AutoDock Vina’s energy function (ADV energy function), during the sampling process. It ranks and selects top candidates based on their predicted high binding affinity. To see a significant improvement in binding affinity, this approach requires generating a large number of sampled ligands for filtering compared to other diffusion-based SBDD methods. This increases the throughput and potentially the computational demands of the sampling process.

Motivated by the limitations of previous methods, we introduce BADGER, **B**inding **A**ffinity **D**iffusion **G**uidance with **E**nanced **R**efinement, a general method for improving ligand binding affinity in diffusion models for SBDD. The core principle of BADGER is to integrate the ADV energy function information directly into the diffusion model’s sampling process using a plug-and-play gradient-guidance approach, without changing the model’s training procedure. This plug-and-play guidance approach ensures that the method is general, flexible, and can be easily adapted to different diffusion-based SBDD methods.

BADGER leverages the information from the ADV energy function to steer the distribution of sampled ligands towards regions of higher binding affinity during the diffusion sampling process. We first model the ADV energy function with a small Equivariant Graph Neural Network (EGNN). We then define a loss function that measures the distance between the EGNN-predicted binding affinity and the desired one. The gradients of this loss function are used to guide the positioning of the ligand during the diffusion sampling process in a manner similar to gradient descent [12, 19, 20]. Our results demonstrate that BADGER achieves state-of-art performance in improving the binding affinity of ligands sampled by diffusion models when benchmarked on CrossDocked2020 [21]. BADGER also offers increased sampling flexibility, as it does not depend on any fragment priors. The code for our paper will be posted at <https://github.com/ASK-Berkeley/BADGER-SBDD>.

Our main contributions can be summarized as follows:

- We introduce BADGER, a diffusion model guidance method designed to enhance the binding affinity of sampled ligands. BADGER exploits the gradient of a binding score function, which is modeled using a trained Equivariant Graph Neural Network (EGNN), to direct the sampling process. The gradient acts similarly to an iterative force

field relaxation, progressively refining the molecular pose towards a desirable high-affinity binding pose during the diffusion sampling process.

- BADGER achieves state-of-the-art performance in all three Vina binding affinity metrics (Vina Score, Vina Min, Vina Dock), surpassing all previous methods in diffusion for SBDD when benchmarked on Cross-Docked2020 [21].
- We also demonstrate that BADGER improves the generated ligand performance on PoseCheck benchmarks [22], improving both the *Redocking Root-Mean-Square-Deviation (RMSD)* and the *Steric Clashes* score. These findings suggest that BADGER not only boosts binding affinity, but also increases the overall validity of the sampled ligands.
- BADGER is a versatile, plug-and-play method that can be easily integrated into different diffusion frameworks utilized in SBDD.

2 Background

We cover the background information of diffusion models, guidance, and their usage in SBDD. We first formally define the problem of enhancing ligand binding affinity to protein pockets within the context of SBDD (§2.1). We then introduce the concept and application of diffusion models for SBDD (§2.2). Finally, we discuss guidance methods and their existing applications in SBDD (§2.3).

2.1 Problem definition

Structure-based Drug Design. Consider a protein pocket with N_p atoms, where each atom is described by N_f feature dimensions. We represent this as a matrix $P = [\mathbf{x}_p, \mathbf{v}_p]$, where $\mathbf{x}_p \in \mathbb{R}^{N_p \times 3}$ represents the Cartesian coordinates of the atoms, and $\mathbf{v}_p \in \mathbb{R}^{N_p \times N_f}$ represents the atom features for atoms that form the protein pocket. We define the operation $[\cdot, \cdot]$ to be concatenation. Let a ligand molecule with N_m atoms, each also described by N_f feature dimensions, be represented as matrix $M = [\mathbf{x}, \mathbf{v}]$, where $\mathbf{x} \in \mathbb{R}^{N_m \times 3}$ and $\mathbf{v} \in \mathbb{R}^{N_m \times N_f}$. The binding affinity between the protein pocket P and the ligand molecule M is denoted by $\Delta G(P, M)$. In the context of SBDD, the goal is to generate ligand M , given a protein pocket P , such that $\Delta G(P, M) < 0$. A more negative value of $\Delta G(P, M)$ indicates a stronger and more favorable binding interaction between the ligand and the protein, which is a desirable property in drug discovery.

Problem of Interest. Building on this background, we are interested in improving the binding affinity $\Delta G(P, M)$, specifically by generating ligands M that achieve a lower $\Delta G(P, M)$ using diffusion-based SBDD methods. In our approach, we use diffusion models tailored for SBDD. Our goal is to develop a guidance strategy for the diffusion model that enables the generation of molecules with higher binding affinity when the guidance is employed, ideally achieving $\Delta G_{guided} < \Delta G_{unguided}$.

2.2 Diffusion Models for Structure-based Drug Design

Recent advancements in generative modeling have been effectively applied to the SBDD task [15, 16, 23]. The development of denoising diffusion probabilistic models [24, 25, 26, 12] has led to approaches in SBDD using diffusion models [6, 13, 18].

In the current literature of diffusion models for SBDD, both protein pockets and ligands are modeled as point clouds. In the sampling stage, protein pockets are treated as the fixed ground truth across all time steps, while ligands start as Gaussian noise and are progressively denoised. This process is analogous to image inpainting tasks, where protein pockets represent the existing parts of an “image,” and ligands are the “missing” parts that need to be filled in. Current approaches typically handle the ligand either as a whole entity [6, 14] or by decomposing ligands into fragments for sampling with pre-imposed priors [13, 18]. In this work, we apply our guidance strategy to both of these methods.

The idea of diffusion-model-based SBDD is to learn a joint distribution between the protein pocket P and the ligand molecule M . The spatial coordinates $x \in \mathbb{R}^{N \times 3}$ and atom features $v \in \mathbb{R}^{N \times K}$ are modeled separately by Gaussian \mathcal{N} and categorical distributions \mathcal{C} , respectively, due to their continuous and discontinuous nature. Here N is the number of atoms and K is the number of element types. The forward diffusion process is defined as follows [6]:

$$q(M_t|M_{t-1}, P) = \mathcal{N}(x_t; \sqrt{1 - \beta_t}x_{t-1}, \beta_t \mathbf{I}) \cdot \mathcal{C}(v_t|(1 - \beta_t)v_{t-1} + \beta_t/K). \quad (1)$$

Here, t is the timestep and ranges from 0 to T , and β_t is the time schedule derived from a sigmoid function. Let $\alpha_t = 1 - \beta_t$ and $\bar{\alpha}_t = \prod_{s=1}^t \alpha_s$. The reverse diffusion process for spatial coordinates x and atom features v is defined as:

$$P(x_{t-1}|x_t, x_0) = \mathcal{N}(x_{t-1}; \tilde{\mu}_t(x_t, x_0), \tilde{\beta}_t \mathbf{I}), \quad (2)$$

$$P(v_{t-1}|v_t, v_0) = \mathcal{C}(v_{t-1}|\tilde{c}_t(v_t, v_0)), \quad (3)$$

where $\tilde{\mu}_t(x_t, x_0) = \frac{\sqrt{\bar{\alpha}_{t-1}}\beta_t}{1-\bar{\alpha}_t}x_0 + \frac{\sqrt{\alpha_t}(1-\bar{\alpha}_{t-1})}{1-\bar{\alpha}_t}x_t$, $\tilde{\beta}_t = \frac{1-\bar{\alpha}_{t-1}}{1-\bar{\alpha}_t}$, and $\tilde{c}_t(v_t, v_0) = c^*(v_t, v_0)/\sum_{k=1}^K c_k^*$, where $c^*(v_t, v_0) = [\alpha_t v_t + (1 - \alpha_t)/K] \odot [\bar{\alpha}_{t-1} v_0 + (1 - \bar{\alpha}_{t-1})/K]$.

2.3 Guidance

Guidance is a key advantage of diffusion models, allowing for iterative adjustment to “guide” the sampled data towards desired properties. This is done by modifying the probability distribution of the sampled space, without the need to retrain the diffusion model. The most basic version of guidance is classifier guidance [12], a plug-and-play method that is straightforward to implement to fine-tune diffusion sampling. Classifier guidance involves decomposing a conditional distribution $P(x_t|y)$ into an unconditional distribution $P(x_t)$ and a classifier term $P(y|x_t)$ through Bayes’ Rule:

$$P(x_t|y) = \frac{P(x_t)P(y|x_t)}{P(y)} \propto P(x_t)P(y|x_t). \quad (4)$$

To understand classifier guidance, consider that at time t , the data distribution in a reverse diffusion process is characterized by a Gaussian distribution:

$$P(x_t|y) = \frac{1}{\sigma_t \sqrt{2\pi}} \exp\left(-\frac{1}{2} \frac{(x_t - \mu_t)^2}{\sigma_t^2}\right). \quad (5)$$

We are interested in maximizing the likelihood that the sampled x_0 belongs to class y . From a score-matching perspective [24, 25], the gradient of the log probability $P(x_t|y)$ with respect to x_t is approximated and simplified through the following steps:

$$\nabla_{x_t} \log P(x_t|y) \approx \nabla_{x_t} \log P(x_t)P(y|x_t), \quad (6)$$

$$= \nabla_{x_t} \log P(x_t) + \nabla_{x_t} \log P(y|x_t), \quad (7)$$

$$= -\frac{1}{\sigma_t} \left(\frac{x_t - \mu_t}{\sigma_t}\right) + \nabla_{x_t} \log P(y|x_t), \quad (8)$$

$$= -\frac{\epsilon_\theta}{\sigma_t} + \nabla_{x_t} \log P(y|x_t), \quad (9)$$

$$= -\frac{1}{\sigma_t} (\epsilon_\theta - \sigma_t \nabla_{x_t} \log P(y|x_t)). \quad (10)$$

The noise term $\epsilon_\theta(x_t, t)$ is parameterized by a denoising network, and $P(y|x_t)$ is modeled by a separately trained classifier. We follow the setup in the Denoising Diffusion Probabilistic Model (DDPM) with $\sigma_t = \sqrt{1 - \bar{\alpha}_t}$ [26]. To implement classifier guidance, we can define a new guided noise term ϵ'_θ :

$$\nabla_{x_t} \log P'(x_t|y) = -\frac{\epsilon'_\theta}{\sigma_t} = -\frac{1}{\sigma_t} (\epsilon_\theta - \sigma_t \nabla_{x_t} \log P(y|x_t)). \quad (11)$$

A scaling factor s is added to control the strength of guidance, and we reach the final expression for classifier guidance:

$$\epsilon'_\theta = \epsilon_\theta - s\sigma_t \nabla_{x_t} \log P_\theta(y|x_t). \quad (12)$$

In the context of SBDD, guidance has been used to control the validity of atoms in generated ligands, thereby indirectly improving ligand-protein binding affinity [13, 27]. Existing works have tried two types of guidance:

1. Using guidance to control the distance of arm fragments and scaffolds to be within a reasonable range [13].
2. Using guidance to prevent clashes between ligand and protein atoms [13, 28, 29].

These methods have shown success in improving ligand-protein binding affinity by indirectly using guidance to improve validity. However, integrating binding affinity guidance into diffusion sampling methods to directly improve binding affinity remains a large gap in the current research landscape.

3 Methods

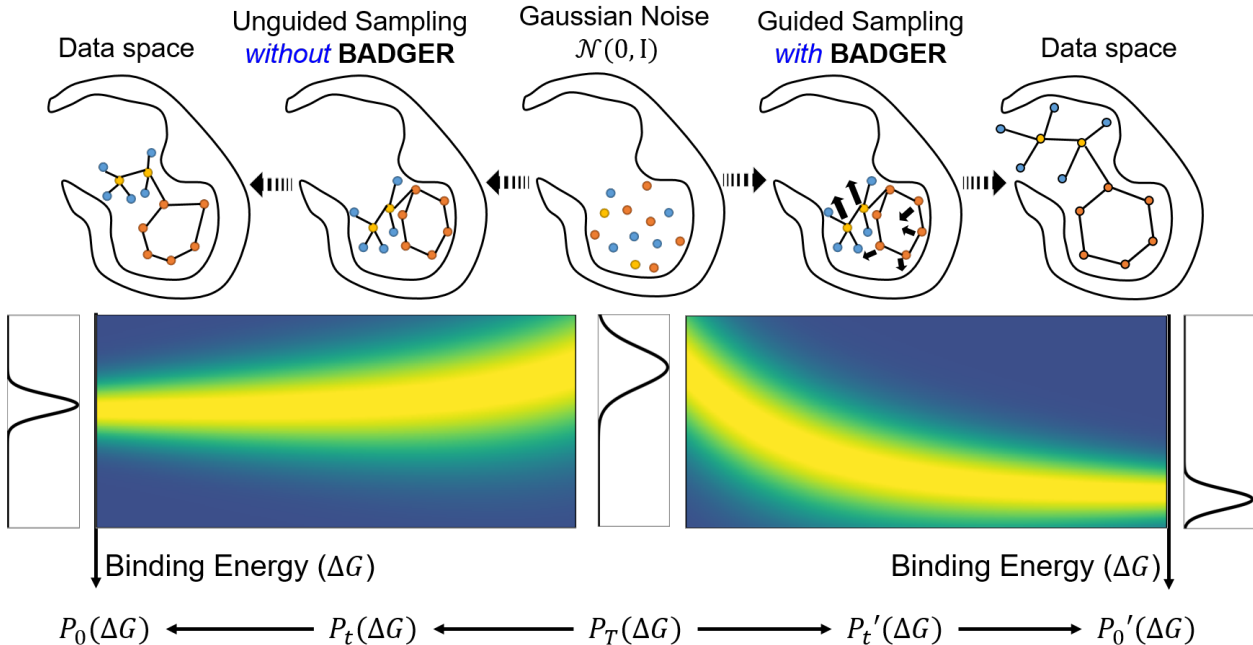


Figure 1: An illustration of **BADGER**, a flexible guidance method that can be added on top of any trained diffusion model. Guided sampling with **BADGER** results in lower protein-ligand binding energies.

We introduce our method: **BADGER** is a plug-and-play, easy-to-use diffusion guidance method for improving ligand-protein pocket binding affinity in SBDD. We include a schematic in Fig. 1. **BADGER** consists of three components:

- (1) **Differentiable Regression Model.** This model acts as an energy function, predicting the binding affinity between ligand and protein pocket pairs (§3.1).
- (2) **Goal-Aware Loss Function.** This loss function is designed to allow the learned energy function to minimize the gap between the predicted binding affinity and the desired binding affinity, helping direct the optimization process towards more favorable interactions (§3.2).

(3) **Guidance Strategy.** Using the gradient of the goal-aware loss function, this strategy iteratively refines the pose of the generated ligand (§3.3).

3.1 Differentiable Regression Model: Building an Energy Function

Consider a ligand-protein pair, where the binding affinity between P and $M = [\mathbf{x}, \mathbf{v}]$ is characterized by ADV energy function $F()$. The binding affinity, ΔG , can be expressed as:

$$\Delta G = F(P, [\mathbf{x}, \mathbf{v}]). \quad (13)$$

The guidance for sampling ligand $[\mathbf{x}, \mathbf{v}]$ given pocket $[\mathbf{x}_p, \mathbf{v}_p]$ depends on the gradient term $\nabla_{\mathbf{x}} \Delta G$. However, the function $F()$ from Autodock Vina is not differentiable. To address this, we use a neural network $f_{\psi}()$ to model $F()$. The predicted binding affinity for a ligand-protein pair can then be expressed as:

$$\Delta G_{predict} = f_{\psi}(P, [\mathbf{x}, \mathbf{v}]). \quad (14)$$

For our regression model, we use a small Equivariant Graph Neural Network (EGNN) [30], due to its efficiency in the sampling process. We provide the full ablation study using different network architectures, including EGNN and the Transformer architecture used in Uni-Mol [31], in §E.

The training of our regression model, referred to here as the ‘‘regressor,’’ uses both the ligand and protein pockets in their ground truth states without any noise. Formally, in the forward diffusion process, the ground truth ligand without noise is denoted as $M_0 = [\mathbf{x}_0, \mathbf{v}_0]$ and the noisy version at timestep t as $M_t = [\mathbf{x}_t, \mathbf{v}_t]$. We train the regressor using M_0 . Since the protein pocket serves as a fixed condition in both training and sampling, we do not introduce noise to the protein pocket P . The full algorithm for training the regressor is detailed in §A.

Unlike the traditional approach of training classifiers on noisy data M_t [12, 32], we simplify the process by training solely on M_0 . This simplification avoids the introduction of additional hyperparameters and complexities associated with selecting sampling time t during classifier training. We show that training on M_0 works well by designing strategies to compute the gradient $\nabla_{\mathbf{x}} \Delta G_{predict}$ for a classifier trained with M_0 . Further discussions on this are found in the next subsection.

3.2 Goal-Aware Loss Function: Guiding the Sampling Process with an Energy Function

Our primary objective is to improve the binding affinity by sampling ligand P with lower ΔG . To achieve this, we design a target energy function, $\mathcal{L}(\Delta G_{predict}, \Delta G_{target})$, to characterize the distance between the predicted binding affinity $\Delta G_{predict}$ and the target binding affinity ΔG_{target} . We use the l_2 norm for the function $\mathcal{L}()$. During sampling, guidance iteratively minimizes $\mathcal{L}(\Delta G_{predict}, \Delta G_{target})$ to steer the binding affinity of sampled ligands towards the desired value ΔG_{target} . The target energy function at each sampling step is expressed as:

$$\mathcal{L}(\Delta G_{predict}, \Delta G_{target}) = \|f_{\psi}(P, [\hat{\mathbf{x}}_0, \hat{\mathbf{v}}_0]) - \Delta G_{target}\|_2. \quad (15)$$

Here, the molecule $\hat{M}_0 = [\hat{\mathbf{x}}_0, \hat{\mathbf{v}}_0]$ is predicted by the dynamic network $\phi_{\theta}()$ at each sampling step in the diffusion model:

$$[\hat{\mathbf{x}}_0, \hat{\mathbf{v}}_0] = \phi_{\theta}([\mathbf{x}_t, \mathbf{v}_t], t, P). \quad (16)$$

To guide the sampling process, we use the gradient of the energy function. We replace the conditional probability term in Eq. 12 with Eq. 15, and the guidance on the noise term is then:

$$\epsilon'_{\theta} = \epsilon_{\theta} + s\sigma_t \nabla_{\mathbf{x}_t} \mathcal{L}(\Delta G_{predict}, \Delta G_{target}). \quad (17)$$

We show the difference between our method and traditional classifier guidance by comparing the gradient calculation between the two methods. For traditional classifier guidance [12], the classifier $f_{\psi}(P, M_t)$ is trained on noisy data M_t . The gradient is calculated by:

$$\nabla_{\mathbf{x}_t} \mathcal{L}(\Delta G_{predict}, \Delta G_{target}) = \nabla_{\mathbf{x}_t} \mathcal{L}(f_{\psi}(P, [\mathbf{x}_t, \mathbf{v}_t]), \Delta G_{target}). \quad (18)$$

Table 1: Summary table of binding affinity performance and other properties for different methods. For each metric, the top two methods are highlighted—**bolded** for the first and underlined for the second. The methods are categorized into three groups: non-Diffusion methods (**non-Diff.**), Diffusion methods (**Diff.**), and Diffusion methods with BADGER (**Diff. + BADGER**).

Metric Group name		Vina Score↓		Vina Min↓		Vina Dock↓		QED↑		SA↑		Diversity↑		High Affinity(%)↑	
		Mean (Δ%)	Med. (Δ%)	Mean (Δ%)	Med. (Δ%)	Mean (Δ%)	Med. (Δ%)	Mean	Med.	Mean	Med.	Mean	Med.	Mean	Med.
Ref.		-6.36	-6.46	-6.71	-6.49	-7.45	-7.26	0.48	0.47	0.73	0.74	-	-	-	-
non-Diff.	liGAN[33]	-	-	-	-	-6.33	-6.20	0.39	0.39	0.59	0.57	0.66	0.67	21.1	11.1
	GraphBP[16]	-	-	-	-	-4.80	-4.70	0.43	0.45	0.49	0.48	0.79	0.78	14.2	6.7
	TacoGFN[34]	-	-	-	-	-8.63	-8.82	0.67	0.67	0.80	0.80	-	-	-	-
	AR[23]	-5.75	-5.64	-6.18	-5.88	-6.75	-6.62	0.51	0.50	0.63	0.63	0.70	0.70	37.9	31.0
	Pocket2Mol[15]	-5.14	-4.70	-6.42	-5.82	-7.15	-6.79	<u>0.56</u>	<u>0.57</u>	<u>0.74</u>	<u>0.75</u>	0.69	0.71	48.4	51.0
Diff.	IPDiff[35]	-6.42	-7.01	-7.45	-7.48	-8.57	-8.51	0.52	0.53	0.61	0.59	0.74	0.73	69.5	75.5
	BindDM[36]	-5.92	-6.81	-7.29	-7.34	-8.41	-8.37	0.51	0.52	0.58	0.58	0.75	0.74	64.8	71.6
	TargetDiff[6]	-5.47	-6.30	-6.64	-6.83	-7.80	-7.91	0.48	0.48	0.58	0.58	0.72	0.71	58.1	59.1
	DecompDiff Ref[13]	-4.97	-4.88	-6.07	-5.79	-7.34	-7.06	0.45	0.45	0.64	0.63	0.82	0.84	64.6	75.5
	DecompDiff Beta[13]	-4.18	-5.89	-6.77	-7.31	<u>-8.93</u>	<u>-9.05</u>	0.29	0.26	0.52	0.52	0.67	0.68	77.7	95.1
Diff. + BADGER	TargetDiff + BADGER	-7.70 (+40.8%)	-8.53 (+35.4%)	<u>-8.33 (+25.5%)</u>	<u>-8.44 (+23.6%)</u>	-8.91 (+14.2%)	-8.84 (+11.8%)	0.46	0.46	0.50	0.49	0.78	0.80	70.2	76.8
	DecompDiff Ref + BADGER	-6.05 (+21.7%)	-6.00 (+23.0%)	-6.75 (+11.2%)	-6.51 (+12.4%)	-7.56 (+3.0%)	-7.41 (+5.0%)	0.45	0.46	0.61	0.60	<u>0.81</u>	<u>0.82</u>	<u>71.1</u>	<u>75.9</u>
	DecompDiff Beta + BADGER	<u>-6.73 (+61.0%)</u>	<u>-8.02 (+36.1%)</u>	-8.46 (+25.0%)	-8.81 (+20.6%)	-9.64 (+7.9%)	-9.71 (+7.3%)	0.30	0.26	0.49	0.49	0.67	0.66	83.7	98.1

Table 2: We benchmark binding affinity performance with DecompOpt [18] on the same test set with 100 pockets. To compare with DecompOpt and TargetDiff w/ Opt. under the same conditions, we sample 100 ligands for each pocket. We then select the top 20 candidates to compute the final binding affinity performance.

Method Metric		Vina Score		Vina Min		Vina Dock	
		Mean (Δ%)	Med (Δ%)	Mean (Δ%)	Med (Δ%)	Mean (Δ%)	Med (Δ%)
Diff.	TargetDiff	-8.70	-8.72	-9.28	-9.25	-9.93	-9.91
	DecompDiff Beta [13]	-6.33	-7.56	-8.50	-8.88	-10.37	-10.05
Diff. + OPT.	TargetDiff w/ Opt. [18]	-7.87	-7.48	-7.82	-7.48	-8.30	-8.15
	DecompOpt [18]	-5.87	-6.81	-7.35	-7.72	-8.98	-9.01
Diff. + BADGER	TargetDiff + BADGER	-10.51 (+33.5%)	-11.12 (+48.6%)	-10.99 (+40.5%)	-11.22 (+50.0%)	-11.33 (+36.5%)	-11.40 (+39.8%)
	DecompDiff Beta + BADGER	-8.66 (+47.5%)	<u>-9.76 (+43.3%)</u>	<u>-10.21 (+38.9%)</u>	<u>-10.53 (+36.4%)</u>	<u>-11.29 (+25.7%)</u>	<u>-11.11 (+23.3%)</u>

In our method, the classifier (or the energy function), $f_\psi(P, M_0)$, is trained on ground truth data M_0 . The gradient term Eq. 17 is calculated through the chain rule:

$$\nabla_{\mathbf{x}_t} \mathcal{L}(\Delta G_{predict}, \Delta G_{target}) = \nabla_{\hat{\mathbf{x}}_0} \mathcal{L}(f_\psi(P, [\hat{\mathbf{x}}_0, \hat{\mathbf{v}}_0]), \Delta G_{target}) \cdot \nabla_{\mathbf{x}_t} \hat{\mathbf{x}}_0. \quad (19)$$

Since the energy function is trained on M_0 , feeding M_0 into $f_\psi()$ is more valid than feeding M_t . However, since the gradient must be taken with respect to \mathbf{x}_t , the chain rule facilitates accurate gradient computation. During our experiments, we found that inputting the combination of $[\hat{\mathbf{x}}_0, \mathbf{v}_t]$ instead of $[\hat{\mathbf{x}}_0, \hat{\mathbf{v}}_0]$ into the energy function yielded better results.

3.3 Guidance Strategy: Binding Affinity Diffusion Guidance with Enhanced Refinement

Finally, integrating all the components, we present Binding Affinity Diffusion Guidance. Recall that we use a Gaussian distribution \mathcal{N} to model the continuous ligand atom coordinates \mathbf{x} . We start with the mean term from §2.2 for a tractable reverse diffusion process conditioned on \mathbf{x}_0 :

$$\tilde{\mu}(\mathbf{x}_t, \mathbf{x}_0) = \frac{\sqrt{\bar{\alpha}_{t-1}}\beta_t}{1 - \bar{\alpha}_t} \mathbf{x}_0 + \frac{\sqrt{\bar{\alpha}_t}(1 - \bar{\alpha}_{t-1})}{1 - \bar{\alpha}_t} \mathbf{x}_t. \quad (20)$$

Using the properties of the diffusion model that allow us to transform from noise to predicted ground truth data [26, 37], we define:

$$\hat{\mathbf{x}}_0 = \frac{1}{\sqrt{\bar{\alpha}_t}} (\mathbf{x}_t - \sqrt{1 - \bar{\alpha}_t} \epsilon_\theta). \quad (21)$$

We can express $\tilde{\mu}_\theta(\mathbf{x}_t, \hat{\mathbf{x}}_0)$ by parameterizing the underlying score network ϕ_θ in Eq. 16 with data $\hat{\mathbf{x}}_0$, rather than the noisy ϵ_θ prediction [38]:

$$\tilde{\mu}_\theta(\mathbf{x}_t, \hat{\mathbf{x}}_0) = \frac{\sqrt{\bar{\alpha}_{t-1}}\beta_t}{1 - \bar{\alpha}_t} \hat{\mathbf{x}}_0 + \frac{\sqrt{\bar{\alpha}_t}(1 - \bar{\alpha}_{t-1})}{1 - \bar{\alpha}_t} \mathbf{x}_t. \quad (22)$$

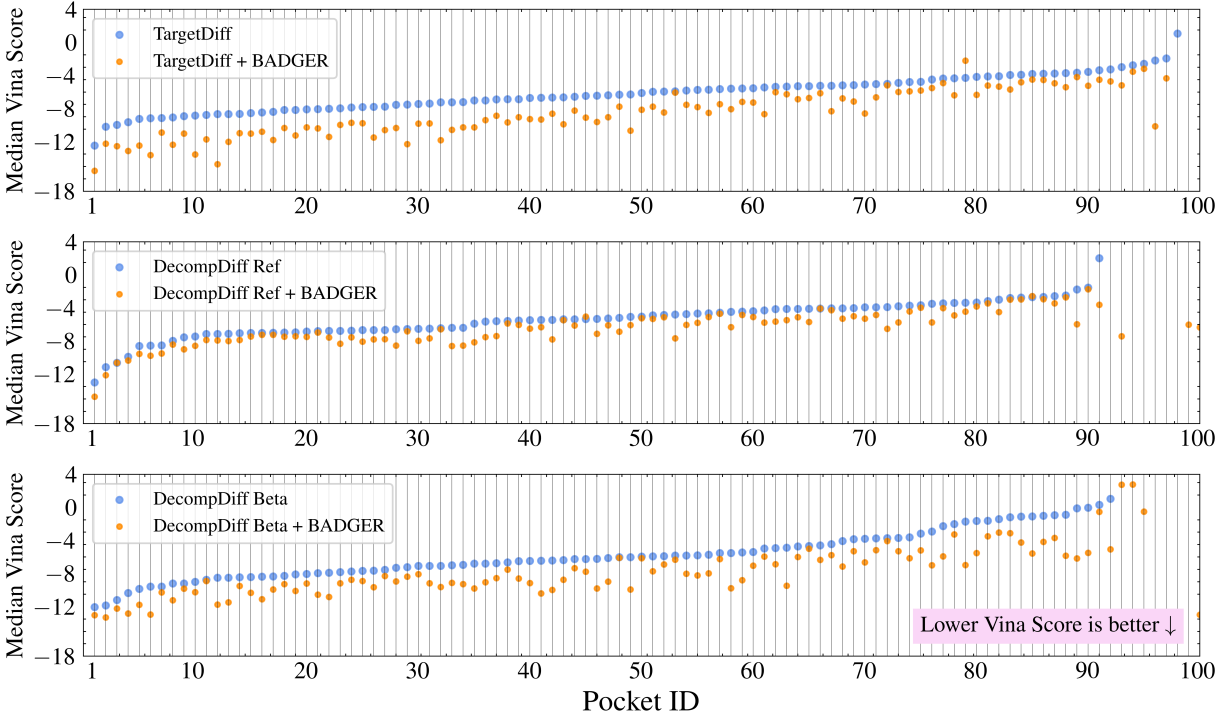


Figure 2: We visualize the improvement in median Vina Score on each of the 100 pockets in the test set for each diffusion model (TargetDiff, DecompDiff Ref, and DecompDiff Beta) after applying BADGER. BADGER improves the median Vina Score for 99% of the protein pockets. For some pockets, the diffusion model score exceeds the range of the y-axis, but BADGER still reduces the score.

We can then express the guided $\tilde{\mu}'_{\theta}(\mathbf{x}_t, \hat{\mathbf{x}}_0)$ with Eq. 17 and Eq. 21 by applying the [guidance term](#) directly to our data prediction:

$$\tilde{\mu}'_{\theta}(\mathbf{x}_t, \hat{\mathbf{x}}_0) = \frac{\sqrt{\bar{\alpha}_{t-1}}\beta_t}{1 - \bar{\alpha}_t} \hat{\mathbf{x}}_0 + \frac{\sqrt{\bar{\alpha}_t}(1 - \bar{\alpha}_{t-1})}{1 - \bar{\alpha}_t} \mathbf{x}_t - \frac{\beta_t}{\sqrt{\alpha_t}} s \nabla_{\mathbf{x}_t} \mathcal{L}(\Delta G_{predict}, \Delta G_{target}). \quad (23)$$

Finally, the guided mean term $\tilde{\mu}'_{\theta}(\mathbf{x}_t, \hat{\mathbf{x}}_0)$ is:

$$\tilde{\mu}'_{\theta}(\mathbf{x}_t, \hat{\mathbf{x}}_0) = \tilde{\mu}_{\theta}(\mathbf{x}_t, \hat{\mathbf{x}}_0) - \frac{\beta_t}{\sqrt{\alpha_t}} s \nabla_{\mathbf{x}_t} \mathcal{L}(\Delta G_{predict}, \Delta G_{target}). \quad (24)$$

Equation 24 is the key equation for BADGER. The intuition is that the guidance seeks to refine the $\tilde{\mu}'_{\theta}(\mathbf{x}_t, \hat{\mathbf{x}}_0)$ of the normal distribution $\mathcal{N}(\mathbf{x}_{t-1}; \tilde{\mu}'_{\theta}(\mathbf{x}_t, \hat{\mathbf{x}}_0), \tilde{\beta}_t \mathbf{I})$ during diffusion sampling such that:

$$\tilde{\mu}'_{\theta}(\mathbf{x}_t, \hat{\mathbf{x}}_0) = \underset{\tilde{\mu}'_{\theta}(\mathbf{x}_t, \hat{\mathbf{x}}_0)}{\operatorname{argmin}} \mathcal{L}(\Delta G_{predict}, \Delta G_{target}). \quad (25)$$

We provide the full algorithm for BADGER in §B, and derivation for Eq. 24 in §C. We also found that applying gradient clipping onto gradient term in Eq. 24 improved the stability of atom coordinates during sampling, and we provide ablations on this in §F.

4 Results and Discussion

We discuss the results from using our guidance method. We first describe the dataset and model baselines that we benchmark against in §4.1. We then present and discuss the results on BADGER’s performance in improving protein-

ligand binding affinity in §4.2. Finally, we analyze the protein-ligand pose quality improvements using BADGER in §4.3.

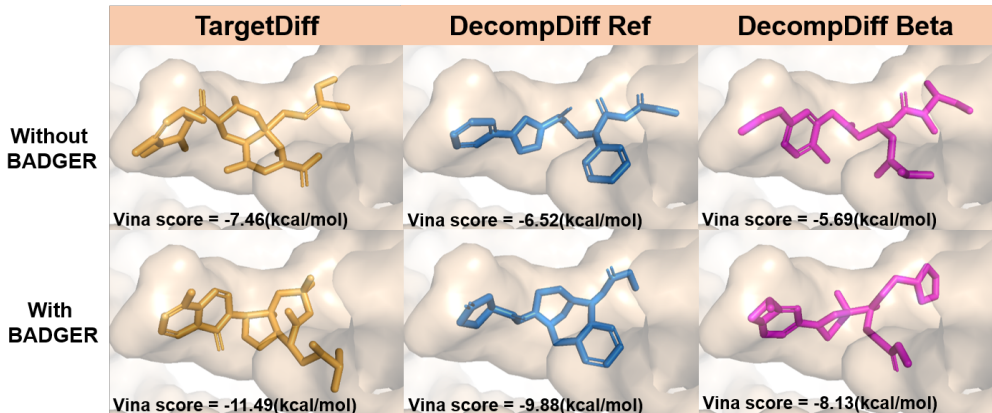


Figure 3: Example ligands sampled from protein pocket “1r1h_A_rec” with TargetDiff, DecompDiff Ref and DecompDiff Beta. For each model, a ligand sampled with BADGER and without BADGER is provided.

4.1 Dataset and Model Baselines

Dataset. We use CrossDocked2020 [21] for all of the experiments. Our data preprocessing and splitting procedures follow the same setting used in TargetDiff and DecompDiff [6, 13]. Following Guan et al. [6], we filter 22.5 million docked protein-ligand complexes based on the criteria of low RMSD for the selected poses ($< 1 \text{ \AA}$) and sequence identity less than 30%. We select 100,000 complexes for training and 100 complexes for testing. For training the regression model used for guidance, both the previous training complexes and the test complexes are included for training. For evaluation, we sample 100 ligands from each pocket, resulting in a total of 10,000 ligands sampled for benchmarking.

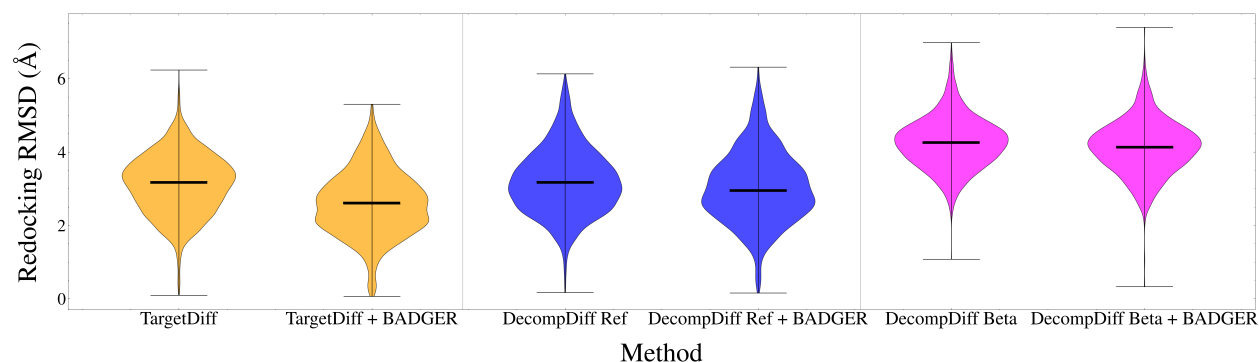
Baselines. We benchmark the performance of our guidance method on top of two state-of-the-art diffusion models for SBDD: **TargetDiff** [6] and **DecompDiff** [13]. For **DecompDiff**, we experiment with two types of priors used in their paper: the reference prior, which we denote as **DecompDiff Ref**, and the pocket prior, which we denote as **DecompDiff Beta**. We include two other SBDD diffusion models as baselines: **IPDiff** [35], and **BindDM** [36]. We also compare **BADGER** with **DecompOpt** [18], an optimization method built for diffusion models for SBDD. Specifically, for **DecompOpt**, we select the groups in Zhou et al. [18]: TargetDiff + Optimization, which we denote as **TargetDiff w/ Opt.**, and DecompDiff + Optimization, which we denote as **DecompOpt**. We also compare our results with non-diffusion SBDD models: **liGAN** [33], **GraphBP** [16], **AR** [23], **Pocket2Mol** [15].

4.2 Binding Affinity Performance and Other Molecular Properties

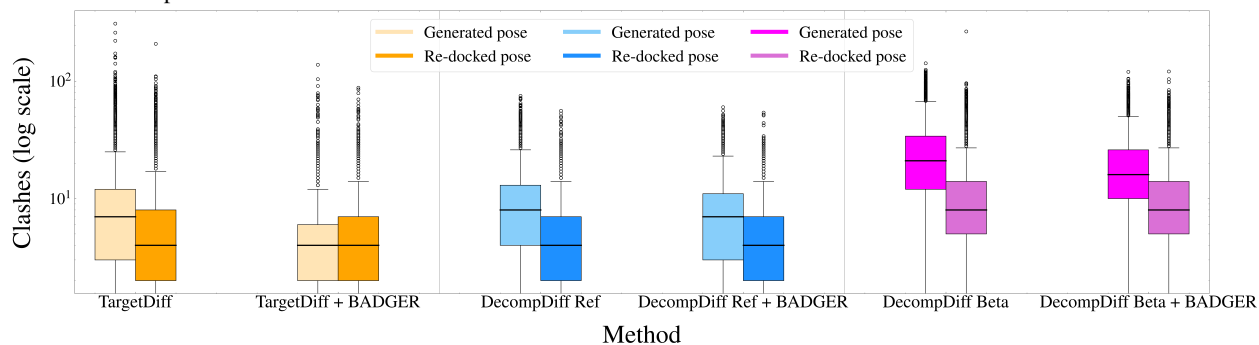
Tab. 1 presents the main metrics for the binding affinity between ligands and the corresponding pocket target. We assess the binding affinity using Autodock Vina [39] through three metrics: **Vina Score**, which is the binding affinity that is directly calculated on the generated pose; **Vina Min**, which is binding affinity calculated on the generated pose with local optimization; and **Vina Dock**, which is binding affinity calculated from the re-docked pose. The results indicate that BADGER outperforms the other diffusion model SBDD methods, achieving improvements of up to 60% in Vina Score, Vina Min, and Vina Dock for TargetDiff, DecompDiff Ref, and DecompDiff Beta. The hyperparameters for the result in Tab. 1 are discussed in §D and §F.

Tab. 2 shows the benchmarking results with DecompOpt [18]. According to Zhou et al. [18], **DecompOpt** and **TargetDiff w/ Opt.** sample 600 ligands for each pocket and select the top 20 candidates filtered by AutoDock Vina. To

compare with these approaches, we sample 100 ligands for each pocket, and select the top 20 candidates to compute the final binding affinity performance. The results show that BADGER outperforms DecompOpt by up to 50% in Vina Score, Vina Min, and Vina Dock. To visualize the improvement in binding affinity for sampled ligands across different



(a) **Violin plots visualization for redocking RMSD.** Lower is better. BADGER improves the generated pose, making it more close to the redocked pose.



(b) **Box plot visualization for the steric clashes score.** Lower is better. BADGER reduces the clashes in the generated ligands and lowers the clashes score.

Figure 4: **Redocking RMSD and Steric Clashes Score improvement with BADGER.** (a) Redocking RMSD plot: lower redocking RMSD indicates that sampled poses have a better agreement with the Vina docking score function. (b) Steric clashes score plot: a lower distributed score means that the sampled poses are more stable. For each method, we evaluate the steric clashes score on the generated pose, which is directly reconstructed from model sampled results, and the redocking pose, which is the pose optimized by AutoDock Vina.

pockets, we plot the median Vina Score for 100 test pockets. This includes comparisons with TargetDiff, DecompDiff Ref, DecompDiff Beta, and the improvement from using BADGER on these models. The results are shown in Fig. 2. The plots show that BADGER effectively improves binding affinity for the different pockets in the test set across all the models. For some challenging pockets, though the median Vina Scores exceed the y-axis range, BADGER still shows improved performance in these instances.

To better understand how BADGER modifies ligand structures to improve the binding affinity between the ligand and protein pocket, we sample some example ligands for the same pocket, “1r1h_A_rec,” with TargetDiff, TargetDiff + BADGER, DecompDiff Ref, DecompDiff Ref + BADGER, DecompDiff Beta, and DecompDiff Beta + BADGER. This is shown in Fig. 3. We note that BADGER tends to guide the ligand structure to be more evenly spread out inside a protein pocket and bind tightly to the pocket.

We also investigate drug likeness, QED [40], and synthesizability, SA [41]. As shown in Tab. 1, BADGER greatly improves the binding affinity while only trading off a small amount on QED and SA score. We put less emphasis on QED and SA score since these are used as a rough filter with a wider acceptable range. Future work could explore

multi-constraint guidance on both the QED and SA score.

4.3 Ligand-Protein Pose Quality

To broaden our evaluation beyond the binding affinity, we assess the quality of generated poses and their potential to enable high-affinity protein-ligand interactions. Following Harris et al. [22], we analyze the redocking RMSD and steric clashes score.

Redocking RMSD. *Redocking RMSD* measures how closely the model-generated ligand pose matches the AutoDock Vina docked pose. A lower redocking RMSD suggests better agreement between the pose before and after redocking, indicating that BADGER more accurately mimics the docking score function. Fig. 4a compares redocking RMSD across models with and without BADGER. The results show that BADGER lowers the RMSD, improving the quality of the ligand poses sampled from diffusion model.

Steric clashes. *Steric clashes* occur when two neutral atoms are closer than their van der Waals radii, leading to energetically unfavorable interactions [42, 43]. The steric clashes score quantifies the number of such clashes in ligand-protein pairs, with a lower score indicating fewer clashes. Fig. 4b shows the steric clashes score for each method, demonstrating that BADGER reduces the number of clashes in the poses generated from TargetDiff, DecompDiff Ref, and DecompDiff Beta.

5 Conclusion

We introduce BADGER, a guidance method to improve the binding affinity of ligands generated by diffusion models in SBDD. BADGER demonstrates that gradient guidance can directly enforce binding affinity awareness into the sampling process of the diffusion model. Our method opens up a new avenue for optimizing ligand properties in SBDD. It is also a general method that can be applied to a wide range of datasets and has the potential to better optimize the drug discovery process. For future work, our approach could potentially be expanded to multi-constraint optimization for ligands in SBDD.

6 Acknowledgement

This work was supported by Laboratory Directed Research and Development (LDRD) funding under Contract Number DE-AC02-05CH11231. We thank Eric Qu, Sanjeev Raja, Toby Kreiman, Rasmus Malik Hoeegh Lindrup and Nithin Chalapathi for their insightful opinions on this work. We also thank Bo Qiang, Bowen Gao, and Xiangxin Zhou for their helpful suggestions on reproducing the benchmark models.

References

- [1] Amy C Anderson. The process of structure-based drug design. *Chemistry & biology*, 10(9):787–797, 2003.
- [2] Tom L Blundell. Structure-based drug design. *Nature*, 384(6604):23, 1996.
- [3] Amr Alhossary, Stephanus Daniel Handoko, Yuguang Mu, and Chee-Keong Kwoh. Fast, accurate, and reliable molecular docking with quickvina 2. *Bioinformatics*, 31(13):2214–2216, 2015.
- [4] Oleg Trott and Arthur J Olson. Autodock vina: improving the speed and accuracy of docking with a new scoring function, efficient optimization, and multithreading. *Journal of computational chemistry*, 31(2):455–461, 2010.
- [5] Thomas A Halgren, Robert B Murphy, Richard A Friesner, Hege S Beard, Leah L Frye, W Thomas Pollard, and Jay L Banks. Glide: a new approach for rapid, accurate docking and scoring. 2. enrichment factors in database screening. *Journal of medicinal chemistry*, 47(7):1750–1759, 2004.
- [6] Jiaqi Guan, Wesley Wei Qian, Xingang Peng, Yufeng Su, Jian Peng, and Jianzhu Ma. 3d equivariant diffusion for target-aware molecule generation and affinity prediction. *arXiv preprint arXiv:2303.03543*, 2023.
- [7] Minkai Xu, Lantao Yu, Yang Song, Chence Shi, Stefano Ermon, and Jian Tang. Geodiff: A geometric diffusion model for molecular conformation generation. *arXiv preprint arXiv:2203.02923*, 2022.
- [8] Emiel Hoogeboom, Victor Garcia Satorras, Clément Vignac, and Max Welling. Equivariant diffusion for molecule generation in 3d. In *International conference on machine learning*, pages 8867–8887. PMLR, 2022.
- [9] Danny Reidenbach and Aditi S Krishnapriyan. Coarsenconf: Equivariant coarsening with aggregated attention for molecular conformer generation. *arXiv preprint arXiv:2306.14852*, 2023.
- [10] Danny Reidenbach. Evosbdd: Latent evolution for accurate and efficient structure-based drug design. In *ICLR 2024 Workshop on Machine Learning for Genomics Explorations*.
- [11] Wenhao Gao and Connor W. Coley. The synthesizability of molecules proposed by generative models. *Journal of Chemical Information and Modeling*, 60(12):5714–5723, 2020.
- [12] Prafulla Dhariwal and Alexander Nichol. Diffusion models beat gans on image synthesis. *Advances in neural information processing systems*, 34:8780–8794, 2021.
- [13] Jiaqi Guan, Xiangxin Zhou, Yuwei Yang, Yu Bao, Jian Peng, Jianzhu Ma, Qiang Liu, Liang Wang, and Quanquan Gu. Decompdiff: diffusion models with decomposed priors for structure-based drug design. 2023.
- [14] Arne Schneuing, Yuanqi Du, Charles Harris, Arian Jamasb, Ilia Igashov, Weitao Du, Tom Blundell, Pietro Lió, Carla Gomes, Max Welling, et al. Structure-based drug design with equivariant diffusion models. *arXiv preprint arXiv:2210.13695*, 2022.
- [15] Xingang Peng, Shitong Luo, Jiaqi Guan, Qi Xie, Jian Peng, and Jianzhu Ma. Pocket2mol: Efficient molecular sampling based on 3d protein pockets. In *International Conference on Machine Learning*, pages 17644–17655. PMLR, 2022.
- [16] Meng Liu, Youzhi Luo, Kanji Uchino, Koji Maruhashi, and Shuiwang Ji. Generating 3d molecules for target protein binding. *arXiv preprint arXiv:2204.09410*, 2022.
- [17] Bowen Gao, Minsi Ren, Yuyan Ni, Yanwen Huang, Bo Qiang, Zhi-Ming Ma, Wei-Ying Ma, and Yanyan Lan. Rethinking specificity in sbdd: Leveraging delta score and energy-guided diffusion. *arXiv preprint arXiv:2403.12987*, 2024.
- [18] Xiangxin Zhou, Xiwei Cheng, Yuwei Yang, Yu Bao, Liang Wang, and Quanquan Gu. Decompopt: Controllable and decomposed diffusion models for structure-based molecular optimization. In *The Twelfth International Conference on Learning Representations*, 2023.

- [19] Fan Bao, Min Zhao, Zhongkai Hao, Peiyao Li, Chongxuan Li, and Jun Zhu. Equivariant energy-guided sde for inverse molecular design. In *The eleventh international conference on learning representations*, 2022.
- [20] Alex Nichol, Prafulla Dhariwal, Aditya Ramesh, Pranav Shyam, Pamela Mishkin, Bob McGrew, Ilya Sutskever, and Mark Chen. Glide: Towards photorealistic image generation and editing with text-guided diffusion models. *arXiv preprint arXiv:2112.10741*, 2021.
- [21] Paul G Francoeur, Tomohide Masuda, Jocelyn Sunseri, Andrew Jia, Richard B Iovanisci, Ian Snyder, and David R Koes. Three-dimensional convolutional neural networks and a cross-docked data set for structure-based drug design. *Journal of chemical information and modeling*, 60(9):4200–4215, 2020.
- [22] Charles Harris, Kieran Didi, Arian R Jamasb, Chaitanya K Joshi, Simon V Mathis, Pietro Lio, and Tom Blundell. Benchmarking generated poses: How rational is structure-based drug design with generative models? *arXiv preprint arXiv:2308.07413*, 2023.
- [23] Shitong Luo, Jiaqi Guan, Jianzhu Ma, and Jian Peng. A 3d generative model for structure-based drug design. *Advances in Neural Information Processing Systems*, 34:6229–6239, 2021.
- [24] Yang Song and Stefano Ermon. Generative modeling by estimating gradients of the data distribution. *Advances in neural information processing systems*, 32, 2019.
- [25] Yang Song, Jascha Sohl-Dickstein, Diederik P Kingma, Abhishek Kumar, Stefano Ermon, and Ben Poole. Score-based generative modeling through stochastic differential equations. *arXiv preprint arXiv:2011.13456*, 2020.
- [26] Jonathan Ho, Ajay Jain, and Pieter Abbeel. Denoising diffusion probabilistic models. *Advances in neural information processing systems*, 33:6840–6851, 2020.
- [27] Jiaqi Guan, Xingang Peng, PeiQi Jiang, Yunan Luo, Jian Peng, and Jianzhu Ma. Linkernet: Fragment poses and linker co-design with 3d equivariant diffusion. *Advances in Neural Information Processing Systems*, 36, 2024.
- [28] Freyr Sverrisson, Jean Feydy, Bruno E Correia, and Michael M Bronstein. Fast end-to-end learning on protein surfaces. In *Proceedings of the IEEE/CVF Conference on Computer Vision and Pattern Recognition*, pages 15272–15281, 2021.
- [29] Octavian-Eugen Ganea, Xinyuan Huang, Charlotte Bunne, Yatao Bian, Regina Barzilay, Tommi Jaakkola, and Andreas Krause. Independent se (3)-equivariant models for end-to-end rigid protein docking. *arXiv preprint arXiv:2111.07786*, 2021.
- [30] Victor Garcia Satorras, Emiel Hoogeboom, and Max Welling. E (n) equivariant graph neural networks. In *International conference on machine learning*, pages 9323–9332. PMLR, 2021.
- [31] Gengmo Zhou, Zhifeng Gao, Qiankun Ding, Hang Zheng, Hongteng Xu, Zhewei Wei, Linfeng Zhang, and Guolin Ke. Uni-mol: A universal 3d molecular representation learning framework. In *The Eleventh International Conference on Learning Representations*, 2023. URL <https://openreview.net/forum?id=6K2RM6wVqKu>.
- [32] Arpit Bansal, Hong-Min Chu, Avi Schwarzschild, Soumyadip Sengupta, Micah Goldblum, Jonas Geiping, and Tom Goldstein. Universal guidance for diffusion models. In *Proceedings of the IEEE/CVF Conference on Computer Vision and Pattern Recognition*, pages 843–852, 2023.
- [33] Matthew Ragoza, Tomohide Masuda, and David Ryan Koes. Generating 3d molecules conditional on receptor binding sites with deep generative models. *Chemical science*, 13(9):2701–2713, 2022.
- [34] Tony Shen, Mohit Pandey, and Martin Ester. Target conditioned GFlowNet for drug design. In *NeurIPS 2023 Generative AI and Biology (GenBio) Workshop*, 2023. URL <https://openreview.net/forum?id=hY1fUTyp6p>.

- [35] Zhilin Huang, Ling Yang, Xiangxin Zhou, Zhilong Zhang, Wentao Zhang, Xiawu Zheng, Jie Chen, Yu Wang, Bin CUI, and Wenming Yang. Protein-ligand interaction prior for binding-aware 3d molecule diffusion models. In *The Twelfth International Conference on Learning Representations*, 2024. URL <https://openreview.net/forum?id=qH9nrMNTIW>.
- [36] Zhilin Huang, Ling Yang, Zaixi Zhang, Xiangxin Zhou, Yu Bao, Xiawu Zheng, Yuwei Yang, Yu Wang, and Wenming Yang. Binding-adaptive diffusion models for structure-based drug design. *arXiv preprint arXiv:2402.18583*, 2024.
- [37] Tim Salimans and Jonathan Ho. Progressive distillation for fast sampling of diffusion models. In *International Conference on Learning Representations*, 2022. URL <https://openreview.net/forum?id=TTdIXIpzhoI>.
- [38] Tuan Le, Julian Cremer, Frank Noe, Djork-Arné Clevert, and Kristof T Schütt. Navigating the design space of equivariant diffusion-based generative models for de novo 3d molecule generation. In *The Twelfth International Conference on Learning Representations*, 2024. URL <https://openreview.net/forum?id=kzGuiRXZrQ>.
- [39] Jerome Eberhardt, Diogo Santos-Martins, Andreas F Tillack, and Stefano Forli. Autodock vina 1.2. 0: New docking methods, expanded force field, and python bindings. *Journal of chemical information and modeling*, 61(8):3891–3898, 2021.
- [40] G Richard Bickerton, Gaia V Paolini, Jérémy Besnard, Sorel Muresan, and Andrew L Hopkins. Quantifying the chemical beauty of drugs. *Nature chemistry*, 4(2):90–98, 2012.
- [41] Peter Ertl and Ansgar Schuffenhauer. Estimation of synthetic accessibility score of drug-like molecules based on molecular complexity and fragment contributions. *Journal of cheminformatics*, 1:1–11, 2009.
- [42] Rosa Buonfiglio, Maurizio Recanatini, and Matteo Masetti. Protein flexibility in drug discovery: from theory to computation. *ChemMedChem*, 10(7):1141–1148, 2015.
- [43] Srinivas Ramachandran, Pradeep Kota, Feng Ding, and Nikolay V Dokholyan. Automated minimization of steric clashes in protein structures. *Proteins: Structure, Function, and Bioinformatics*, 79(1):261–270, 2011.
- [44] Ilia Igashov, Hannes Stärk, Clément Vignac, Victor Garcia Satorras, Pascal Frossard, Max Welling, Michael Bronstein, and Bruno Correia. Equivariant 3d-conditional diffusion models for molecular linker design. *arXiv preprint arXiv:2210.05274*, 2022.
- [45] Diederik P Kingma and Jimmy Ba. Adam: A method for stochastic optimization. *arXiv preprint arXiv:1412.6980*, 2014.

A Algorithm for training regression model

We outline the full algorithm for training our regression model, which is discussed in §3.1.

Algorithm 1 Algorithm for training regression model

Input The protein-ligand binding dataset $\{(P_i, M_i), \Delta G_i\}_{i=1}^N$, a neural network $f_\theta()$
while $f_\theta()$ does not converge **do**
 for $i = \text{shuffle}\{1, 2, 3, 4, \dots, N\}$ **do**
 Predict binding affinity with network $\Delta \hat{G}_i = f_\theta(P_i, M_i)$
 Calculate MSE loss for binding affinity $\mathcal{L} = \|\Delta \hat{G}_i - \Delta G_i\|_2$
 Mask out loss if the ground truth binding affinity is invalid: $\mathcal{L} \leftarrow 0$ if $\Delta G_i > 0$
 update θ base on loss \mathcal{L}
 end for
end while

B Algorithm for guidance sampling

We outline the full algorithm for our guidance sampling method, which is described in §3.3.

Algorithm 2 Sampling Algorithm for BADGER

Input The protein binding pocket P , learned diffusion model ϕ_θ , regression model for binding affinity prediction f_ψ , target binding affinity ΔG_{target} , scale factor on guidance s
Output Sampled ligand molecule M that binds to pocket P
Sample number of atoms in M based on the prior distribution conditioned on pocket size
Move the center of mass of protein pocket P to zero, do the same movement for ligand M
Sample initial molecular atom coordinates x_T and atom types v_T
 $x_T \in \mathcal{N}(0, \mathbf{I})$
 $v_T = \text{one_hot}(\text{argmax}_i(g_i))$, where $g \sim \text{Gumble}(0, 1)$
for t in $T, T-1, \dots, 1$ **do**
 Predict $[\hat{x}_0, \hat{v}_0]$ through $[\hat{x}_0, \hat{v}_0] = \phi_\theta([x_t, v_t], t, P)$
 Calculate guidance $g = \nabla_{x_t} \|f_\psi(P, [\hat{x}_0, \hat{v}_0]) - \Delta G_{target}\|_2$
 $\tilde{\mu}_t(x_t, \hat{x}_0) = \frac{\sqrt{\bar{\alpha}_t - 1} \beta_t}{(1 - \bar{\alpha}_t)} \hat{x}_0 + \frac{\sqrt{\bar{\alpha}_t (1 - \bar{\alpha}_{t-1})}}{(1 - \bar{\alpha}_t)} x_t$
 Apply guidance:
 $\tilde{\mu}'_t(x_t, \hat{x}_0) = \tilde{\mu}_t(x_t, \hat{x}_0) - s \frac{\beta_t}{\sqrt{\alpha_t}} g$
 $\tilde{\beta}_t = \frac{1 - \bar{\alpha}_{t-1}}{1 - \bar{\alpha}_t} \beta_t$
 sample $\epsilon \sim \mathcal{N}(0, \mathbf{I})$
 $x_{t-1} = \epsilon \sqrt{\tilde{\beta}_t} + \tilde{\mu}'_t(x_t, \hat{x}_0)$
 Sample v_{t-1} from $q_\theta(v_{t-1}|v_t, \hat{v}_0) = \mathcal{C}(v_{t-1}|\tilde{c}(v_t, v_0))$
 $\tilde{c}(v_t, v_0) = (\alpha_t v_t + (1 - \alpha_t)/K) \odot (\bar{\alpha}_{t-1} v_0 + (1 - \bar{\alpha}_{t-1})/K)$
 Sample v_{t-1}
 $v_{t-1} = \text{argmax}(\tilde{c}(v_t, v_0))$
end for

C Full derivation for the guidance term

We provide the full derivation for our method, as described in §3.3. We start with a tractable reverse diffusion process that conditions on x_0 :

$$P(\mathbf{x}_{t-1}|\mathbf{x}_t, \mathbf{x}_0) = \mathcal{N}(\mathbf{x}_{t-1}; \tilde{\mu}(\mathbf{x}_t, \mathbf{x}_0), \tilde{\beta}_t \mathbf{I}), \quad (26)$$

$$\text{where } \tilde{\mu}(\mathbf{x}_t, \mathbf{x}_0) = \frac{\sqrt{\bar{\alpha}_{t-1}}\beta_t}{1 - \bar{\alpha}_t} \mathbf{x}_0 + \frac{\sqrt{\bar{\alpha}_t}(1 - \bar{\alpha}_{t-1})}{1 - \bar{\alpha}_t} \mathbf{x}_t \text{ and } \tilde{\beta}_t = \frac{1 - \bar{\alpha}_{t-1}}{1 - \bar{\alpha}_t} \beta_t. \quad (27)$$

We can express $\tilde{\mu}_\theta(\mathbf{x}_t, \hat{\mathbf{x}}_0)$ as follows:

$$\tilde{\mu}_\theta(\mathbf{x}_t, \hat{\mathbf{x}}_0) = \tilde{\mu}(\mathbf{x}_t, \frac{1}{\sqrt{\bar{\alpha}_t}}(\mathbf{x}_t - \sqrt{1 - \bar{\alpha}_t}\boldsymbol{\epsilon}_\theta)), \quad (28)$$

$$= \frac{\sqrt{\bar{\alpha}_{t-1}}\beta_t}{1 - \bar{\alpha}_t} \frac{1}{\sqrt{\bar{\alpha}_t}}(\mathbf{x}_t - \sqrt{1 - \bar{\alpha}_t}\boldsymbol{\epsilon}_\theta) + \frac{\sqrt{\bar{\alpha}_t}(1 - \bar{\alpha}_{t-1})}{1 - \bar{\alpha}_t} \mathbf{x}_t \quad (29)$$

We can then express the guided $\tilde{\mu}'_\theta(\mathbf{x}_t, \hat{\mathbf{x}}_0)$ with Eq. 17 and Eq. 21:

$$\tilde{\mu}'_\theta(\mathbf{x}_t, \hat{\mathbf{x}}_0) = \frac{\sqrt{\bar{\alpha}_{t-1}}\beta_t}{1 - \bar{\alpha}_t} \frac{1}{\sqrt{\bar{\alpha}_t}}(\mathbf{x}_t - \sqrt{1 - \bar{\alpha}_t}\boldsymbol{\epsilon}'_\theta) + \frac{\sqrt{\bar{\alpha}_t}(1 - \bar{\alpha}_{t-1})}{1 - \bar{\alpha}_t} \mathbf{x}_t, \quad (30)$$

$$= \frac{\sqrt{\bar{\alpha}_{t-1}}\beta_t}{1 - \bar{\alpha}_t} \frac{1}{\sqrt{\bar{\alpha}_t}}(\mathbf{x}_t - \sqrt{1 - \bar{\alpha}_t}\boldsymbol{\epsilon}_\theta) + \frac{\sqrt{\bar{\alpha}_t}(1 - \bar{\alpha}_{t-1})}{1 - \bar{\alpha}_t} \mathbf{x}_t - \frac{\beta_t}{\sqrt{\bar{\alpha}_t}} s \nabla_{\mathbf{x}_t} \mathcal{L}(\Delta G_{predict}, \Delta G_{target}), \quad (31)$$

$$= \tilde{\mu}_\theta(\mathbf{x}_t, \hat{\mathbf{x}}_0) - \frac{\beta_t}{\sqrt{\bar{\alpha}_t}} s \nabla_{\mathbf{x}_t} \mathcal{L}(\Delta G_{predict}, \Delta G_{target}) \quad (32)$$

D Implementation details

We provide further details on our implementation for the different components of our method. The regression models are discussed in §3.1.

Parameters for EGNN Regression Model. The Equivariant Graph Neural Network (EGNN) is built based on Igashov et al. [44]. The model contains two equivariant graph convolution layers. The total number of parameters for the model is 0.3 million.

Training EGNN. The EGNN is trained using Adam [45], with learning rate = $5e^{-4}$, weight decay = 0, $\beta_1 = 0.95$, and $\beta_2=0.999$. We use the ReduceLROnPlateau scheduler with decaying factor = 0.5, patience = 2 and minimum learning rate = $1e^{-6}$. We use a Mean Squared Error (MSE) loss. We train the model for 20 epochs, and the loss drop down to 0.1. For the loss, we apply loss masking to get rid of the invalid data. Specifically, for any data with a ground truth binding affinity > 0 kcal/mol, we set the loss for this data to be zero during training.

Parameters for Transformer Regression Model. The Transformer is built based on Zhou et al. [31]. The model contains 10 attention layers. The total number of parameters for the model is 2.9 million.

Training the Transformer. The Transformer is trained by using Adam [45], with learning rate = $5e^{-4}$, weight decay = 0, $\beta_1 = 0.95$, and $\beta_2=0.999$. We use ReduceLROnPlateau scheduler with decaying factor = 0.5, patience = 2 and minimum learning rate = $1e^{-6}$. We use a Mean Squared Error (MSE) loss. We train the model for 20 epochs, and the loss drop down to 0.02. For the loss, we apply loss masking to get rid of the invalid data. Specifically, for any data with a ground truth binding affinity > 0 kcal/mol, we set the loss for this data to be zero during training.

Parameters for the Diffusion Model. We use the pre-trained checkpoint of the diffusion model from Guan et al. [6] and Guan et al. [13] for TargetDiff and DecompDiff, respectively. We apply our guidance method on top of these trained models.

Diffusion Sampling with Guidance. During the sampling, we apply guidance with a certain combination of the scale factor and ΔG_{target} . We apply clipping to the term $\frac{\beta_t}{\sqrt{\alpha_t}} s \nabla_{\mathbf{x}_t} \mathcal{L}(\Delta G_{predict}, \Delta G_{target})$ in Eq. 24 to improve the stability of the sampling process. The hyperparameters for the results in Tab. 1 (§4.2) are reported in Tab. 3.

Diffusion sampling takes 1000 steps. For "DecompDiff Ref + BADGER" and "DecompDiff Beta + BADGER," we report the metric for the results at sampled steps = 1000. For "TargetDiff + BADGER," we employ early stopping and report the results at sampled steps = 960.

Table 3: Scale factors and ΔG_{target} for the experiments reported in Tab. 1.

Methods	Scale factor	ΔG_{target} (kcal/mol)	Clipping
TargetDiff + BADGER	80	-16	1
DecompDiff Ref + BADGER	100	-40	0.003
DecompDiff Beta + BADGER	100	-40	0.003

GPU information. All the experiments are conducted on an NVIDIA RTX 6000 Ada Generation.

Benchmark score calculations. We calculated QED, SA, and binding affinity using the same code base as in Guan et al. [6]. Diversity is calculated as follows for the sampled ligands, following Guan et al. [6, 13]:

$$Diversity = \frac{1}{n} \sum_n^1 (1 - pairwise\ Tanimoto\ similarity). \quad (33)$$

E Ablation on different types of regression models

We provide an ablation on the regression model discussed in §3.1, and look at the EGNN and Transformer architectures in Tab. 4.

Table 4: Ablation on the effect of the type of regression model on the same pocket, and under the same scale factor = 80, target binding affinity $\Delta G_{target} = -20$ kcal/mol, and gradient clipping= $5e-3$.

Regression Model	Vina Score		Vina Min		Vina Dock		QED		SA	
	Mean	Med	Mean	Med	Mean	Med	Mean	Med	Mean	Med
No BADGER	-3.47	-3.36	-3.77	-3.79	-4.45	-4.29	0.45	0.45	0.71	0.70
BADGER with EGNN	-4.88	-4.87	-4.86	-4.87	-5.10	-4.98	0.39	0.40	0.63	0.66
BADGER with Transformer	-3.74	-3.64	-3.96	-3.81	-3.79	-4.36	0.39	0.41	0.68	0.69

F Effects of gradient clipping

We expand on the results in §4.2 and provide a study on the effect of gradient clipping on one single pocket for TargetDiff + BADGER, DecompDiff Ref + BADGER, DecompDiff Beta + BADGER in Tab. 5, Tab. 6, and Tab. 7. We find that gradient clipping can reduce an atom moving away from the center of the mass, caused by large gradients at early sampling steps. Thus, it can improve the stability of the sampling process and enhance the binding affinity and molecule validity.

Table 5: Study on the effect of gradient clipping on the same pocket with TargetDiff, with scale factor(s) = 100, target binding affinity $\Delta G_{target} = -40\text{kcal/mol}$.

Clip	Vina Score		Vina Min		Vina Dock		QED		SA	
	Mean	Med	Mean	Med	Mean	Med	Mean	Med	Mean	Med
1e-1	-4.00	-4.18	-3.64	-3.74	-4.69	-4.81	0.38	0.37	0.67	0.68
1e-2	-4.63	-4.56	-4.67	-4.47	-5.11	-4.82	0.39	0.37	0.62	0.64
1e-3	-4.18	-4.01	-4.22	-4.09	-4.67	-4.51	0.43	0.45	0.68	0.69

Table 6: Study on the effect of gradient clipping on the same pocket with DecomDiff Ref, with scale factor(s) = 100 and target binding affinity $\Delta G_{target} = -40\text{kcal/mol}$.

Clip	Vina Score		Vina Min		Vina Dock		QED		SA	
	Mean	Med	Mean	Med	Mean	Med	Mean	Med	Mean	Med
1	-6.56	-6.65	-6.24	-6.69	-6.61	-6.78	0.46	0.48	0.49	0.50
1e-1	-6.36	-6.40	-6.20	-6.51	-6.60	-6.71	0.48	0.48	0.49	0.50
1e-2	-5.37	-5.48	-5.82	-5.91	-6.39	-6.41	0.45	0.44	0.55	0.56
1e-3	-4.30	-4.37	-4.84	-4.92	-5.71	-5.73	0.55	0.56	0.65	0.65

Table 7: Study on the effect of gradient clipping on the same pocket with DecomDiff Beta, with scale factor(s) = 100 and target binding affinity $\Delta G_{target} = -40\text{kcal/mol}$.

Clip	Vina Score		Vina Min		Vina Dock		QED		SA	
	Mean	Med	Mean	Med	Mean	Med	Mean	Med	Mean	Med
1	-5.86	-5.93	-6.50	-6.68	-8.03	-8.23	0.45	0.46	0.31	0.30
1e-1	-5.13	-5.10	-6.21	-6.40	-7.84	-7.83	0.35	0.34	0.29	0.28
1e-2	-7.74	-7.76	-8.23	-8.18	-8.74	-8.69	0.43	0.43	0.37	0.36
1e-3	-3.80	-4.15	-6.15	-6.09	-6.96	-7.22	0.42	0.43	0.48	0.50